

# Computer simulation of texture evolution during grain growth: effect of boundary properties and initial microstructure

N. Ma, A. Kazaryan, S.A. Dregia, Y. Wang \*

*Department of Materials Science and Engineering, The Ohio State University, 2041 College Road,  
177 Watts Hall, Columbus, OH 43210-1178, USA*

Received 13 March 2004; received in revised form 1 May 2004; accepted 4 May 2004  
Available online 4 June 2004

## Abstract

We investigate orientation selection during grain growth by computer simulation in two-dimension using the phase-field method. The model characterizes misorientation in three-dimension with all three degrees of freedom. The systems considered consist of a single cube component embedded in a matrix of randomly oriented grains in the initial microstructure. The average grain size and size distribution are similar for both textured and randomly oriented grains. Starting from various fractions and spatial distributions of the cube component, we show that the effect of boundary energy anisotropy on texture development differs drastically from that of mobility anisotropy. In all cases the fraction of the cube component increases if boundary energy is anisotropic, and decreases if boundary mobility is anisotropic while energy is isotropic. Similar to previous studies, when boundary energy is anisotropic the misorientation distribution is no longer time-invariant and grain growth kinetics deviates from the behavior of isotropic grain growth. However, mobility anisotropy could also alter misorientation distribution and hence affect grain growth kinetics, which is different from the results obtained previously for systems of either random or single-component texture. The initial spatial distribution of the texture component plays an important role in determining the time-evolution of the misorientation distribution and hence affects the overall kinetics of texture evolution and grain growth. The simulation results are analyzed using Turbull's theory on grain growth. It is found that even though many individual factors affect texture evolution during grain growth, the key factor that really controls the process is the local grain boundary energy density.

© 2004 Acta Materialia Inc. Published by Elsevier Ltd. All rights reserved.

**Keywords:** Texture development; Grain growth; Anisotropy; Phase-field; Computer modeling

## 1. Introduction

There is an important interdependence between anisotropy and preferred orientation (or texture), not only in the performance but also in the processing of materials. Controlling texture is often necessary for optimizing the physical properties of a polycrystalline aggregate, especially when those properties are highly anisotropic in the individual crystals. But the extent of texture itself is dependent on the anisotropy in properties of boundaries between crystals, and it may increase or decrease as boundaries migrate to grow certain orientations at the expense of others. The structure and

composition of grain boundaries and hence their properties may vary significantly from one boundary to another because of the variation in crystallographic misorientation and boundary plane inclination [1,2]. The relative abundance of different types of grain boundaries is determined by the degree of texture and by the spatial distribution of texture components introduced by processes such as deposition, deformation, transformation, recrystallization and grain growth [3,4]. Texture development has been a topic of intense research for more than five decades [5–8]. Recently, with advances in experimental characterization, e.g., orientation mapping (OIM) [9], and computer simulations [10–21], there has been an increasing interest in advancing our fundamental understanding of the mechanisms underlying grain orientation selection during

\* Corresponding author. Fax: +1-614-292-1537.  
E-mail address: [wang.363@osu.edu](mailto:wang.363@osu.edu) (Y. Wang).

thermal and mechanical processing. In this study, we focus on texture evolution during grain growth.

Texture development during grain growth has been studied mainly through statistical modeling and Monte Carlo (MC) simulations [10–19,22–24]. For example, Abbruzzese and Lücke [22] studied interactions between two texture components by extending Hillert's statistical model of grain growth [25]. For simplicity, they considered two types of grain orientations (or texture components) A and B with three types of grain boundaries (A–A, B–B and A–B). Accounting for anisotropy only in boundary mobility, with high mobility for A–B and low mobility for A–A and B–B boundaries, they have shown that the minority component should grow at the expense of the majority component, leading to oscillations in the volume fractions of the two texture components. Such a phenomenon has been observed by Mehnert and Klimanek [14,15] and by Ivasishin et al. [16] in their Monte Carlo simulations.

Different from Abbruzzese and Lücke [22], Novikov studied the evolution of a single texture component (A) in a matrix of randomly orientated grains (B) [23]. In Novikov's statistical analysis, both A–B and B–B boundaries were assumed to have high energy and high mobility, and it was concluded that the fraction of the texture grains (in this case, the A grains) decreases unless their initial average size was much larger than that of the matrix B grains. Hwang et al. [13] used MC simulations to study a system similar to Novikov's, but they allowed for anisotropy only in boundary energy. They observed a marked growth of the texture component even when the textured grains did not have an initial size advantage. Recently Rollett [19] also investigated evolution of a single cube-texture component in a matrix of randomly oriented grains using the MC method. He employed two sets of functions for misorientation dependence of mobility and energy, and found that the texture evolution was sensitive to the mobility function but not to the energy function.

It is apparent that many factors affect texture evolution during grain growth, including the number of texture components and degree of texturing, initial volume fractions, grain sizes and size distributions of different texture components, and anisotropy in grain boundary energy and mobility. In addition, the spatial distribution of the texture component in the initial microstructure should also be an important factor because the spatial distribution affects directly the misorientation distribution function (MDF). To better understand the individual and combined effects of these factors, it seems necessary to distinguish the roles played by each of them and, most importantly, to identify the key parameter or parameters that control the texture evolution.

In this article, we examine systematically the individual and combined effects of anisotropy in boundary energy and mobility, and initial microstructure on the

evolution of a texture component in a matrix of randomly oriented grains. The simulated systems consist of a single cube component (with 5° spread around the cube orientation) embedded in a matrix of randomly oriented grains with misorientations following the Mackenzie distribution. Systems containing more than one texture component will be investigated in a separate paper. The average grain size and size distributions of the textured and randomly oriented grains are similar in the initial microstructures. The misorientation is characterized in three-dimension with all three degrees of freedom. Two initial fractions (12.5% and 27%) and three different initial dispersions of the texture grains are considered (random, uniform and highly clustered).

Independent of texture evolution, extensive work has been done in modeling the effect of anisotropy in grain boundary energy and mobility on the morphology of a polycrystalline microstructure and the kinetics of coarsening during grain growth [18,20,21]. It has been demonstrated [20,21] that starting with either a single-component texture or a random texture, anisotropy in boundary mobility plays little role while anisotropy in boundary energy strongly modifies both the morphology and the kinetics of grain growth. However, the conclusions drawn from the previous studies may not apply to the systems considered in the current study, where the starting orientation distribution function (ODF) and MDF will depend on the fraction and dispersion of the textured grains, which are both time-dependent. It will be shown that when a certain fraction of a texture component exists in a matrix of randomly oriented grains, both boundary energy and mobility anisotropy may have profound influences on grain growth in general and texture development in particular.

We will limit our scope of study to bulk materials in this article. For sheets and thin films, additional factors, not considered here, may contribute to orientation selection during grain growth, such as anisotropy in surface energy and film/substrate interfacial energy, surface grooving drag and thermal or epitaxial stresses in the films. Consideration of these factors is straightforward in the phase-field model employed, and they will be examined in a separate article.

## 2. Method

### 2.1. Phase-field method

The phase-field method (PFM) for grain growth has been developed along two independent lines: one involves multiple orientation fields [26,27] and the other employs a single orientation field [28,29]. In the current study, we employ the former approach and characterize misorientations in three-dimension with all three degrees of freedom. Orientations of grains are represented by

Euler angles [30] whose values are assigned to each grain according to the desired orientation distribution. The misorientation of two adjacent grains is then determined from their Euler triplets. In the simulation, we calculate all the possible misorientation angles from two Euler triplets by symmetry operations of the crystal. We then follow the convention [31,32] to assign the minimum misorientation angle to the grain boundary, known also as the *disorientation* [31,32]. In this study we ignore the dependence of grain boundary properties on inclination and rotation axis. Therefore, the misorientation angle of a boundary uniquely determines the boundary energy and mobility (see e.g., Fig. 1). Below, we give a brief introduction to the phase-field method. Detailed descriptions of the method for simulations of grain growth phenomena in general and grain growth in anisotropic media in particular can be found in [20,26].

In the multiple orientation PFM, the microstructure of an arbitrary polycrystalline material is described by a set of non-conserved long-range order (lro) parameters ( $\eta_1, \eta_2, \dots, \eta_p$ ) with each of them describing a specific crystallographic orientation of the grains. The evolution of the system is described by the time-dependent Ginzburg–Landau equation

$$\frac{\partial \eta_i}{\partial t} = -L \frac{\delta F}{\delta \eta_i}, \quad (1)$$

where  $L$  is the kinetic coefficient that characterizes grain boundary mobility and  $F$  is the total free energy of the system. In gradient thermodynamics [33], the total free energy is expressed on a coarse-grained level as

$$F = \int [f_0(\eta_i) + \kappa(\nabla \eta_i)^2] dv, \quad (2)$$

where  $\kappa$  is the gradient energy coefficient and  $f_0$  is the local free energy. The exact form of  $f_0$  is not important as long as it provides degenerate minima corresponding

to each grain orientation,  $\eta_i$ . A simple form that satisfies this requirement is

$$f_0 = \frac{a}{2} \sum_{i=1}^P \left( -\eta_i^2 + \frac{1}{2} \eta_i^4 \right) + \sum_{i=1}^P \sum_{j>i}^P \frac{b}{4} \eta_i^2 \eta_j^2, \quad (3)$$

where  $P$  is the total number of lro parameters in the system,  $a$  and  $b$  are phenomenological parameters with their values determined by grain boundary energy and width.

When  $L$ ,  $\kappa$ ,  $a$  and  $b$  are assumed constant, the above equations describe isotropic grain growth [26]. The dependency of grain boundary properties on misorientation in this study is introduced by making  $L$ ,  $\kappa$  and  $b$  misorientation-dependent under the constraint of constant grain boundary width [20]. Since the phase-field method is a non-boundary tracking approach, one needs to describe the misorientations of grain boundaries through the field variables,  $\eta_i$ . Even though there are many different ways of doing so, we employ in the current study the following simple function to characterize the misorientation field corresponding to an arbitrary distribution of grain boundaries in the system

$$\theta(\mathbf{r}) = \frac{\sum_{i,j \neq i}^P \eta_i^2 \eta_j^2 \theta_{ij}}{\sum_{i,j \neq i}^P \eta_i^2 \eta_j^2}, \quad (4)$$

where  $\theta_{ij}$  is the misorientation angle between grain  $i$  and  $j$  with orientations  $\eta_i$  and  $\eta_j$ . Eq. (4) assigns a constant misorientation angle within the grain boundary region between grain  $i$  and grain  $j$ , with the value of the angle  $\theta_{ij}$  given by a predetermined look-up table, and yields a weighted-mean misorientation at junctions.

The grain boundary energy anisotropy is characterized by a plateau for high-angle boundaries and by the Read–Shockley formula for small angle boundaries [34]

$$\gamma(\theta) = \begin{cases} \gamma_0 \frac{\theta}{\theta_m} \left( 1 - \ln \frac{\theta}{\theta_m} \right) & \theta < \theta_m, \\ \gamma_0 & \theta \geq \theta_m, \end{cases} \quad (5)$$

where  $\theta_m$  is the maximum angle at which the Read–Shockley equation still holds, and  $\gamma_0$  is a constant. Correspondingly, the mobility anisotropy is characterized by [35]

$$L(\theta) = \begin{cases} L_0 \left( \frac{\theta}{\theta_m} \right)^5 & \theta < \theta_m, \\ L_0 & \theta \geq \theta_m. \end{cases} \quad (6)$$

Note that the magnitude of  $\theta_m$  determines the degree of anisotropy and it is assumed to be  $20^\circ$  in the simulations. The dependences of boundary energy and mobility described by Eqs. (5) and (6) are shown in Fig. 1.

## 2.2. Initial microstructure

The initial microstructure (Fig. 2(a)) employed in the current study is obtained from nucleation and growth of

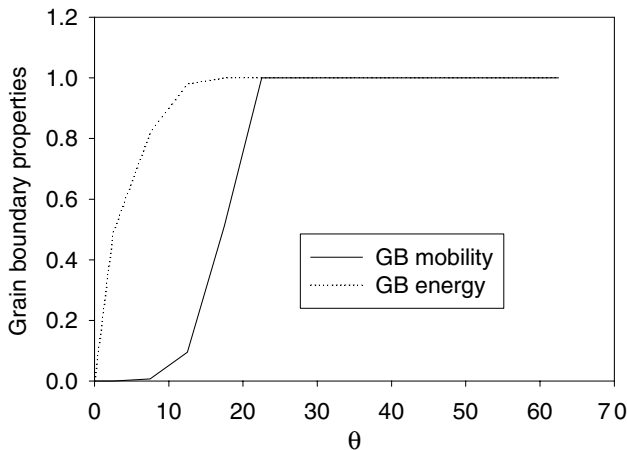


Fig. 1. Dependency of boundary energy and mobility on misorientation described by Eqs. (5) and (6).

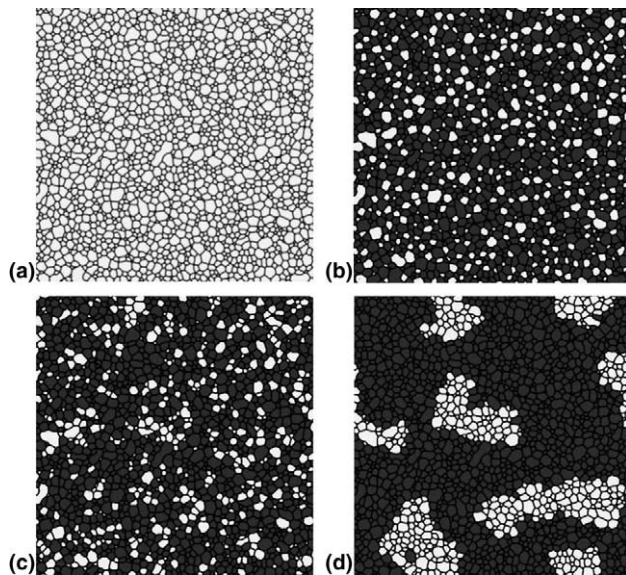


Fig. 2. Initial microstructures with various dispersions of the texture component. (a) Starting microstructure before assigning preferred orientations; (b)–(c) uniform, random and clustered dispersions of the texture component, with light shade representing grains of preferred orientations (within  $5^\circ$  from (000) in Euler space) and dark shade representing randomly oriented grains.

small crystals out of liquid, using a phase-field simulation with random fluctuations of the  $I_{ro}$  parameters. Both interface and grain boundary properties are assumed isotropic at this stage. Texture is introduced into the solidified microstructure by assigning orientations to individual grains, with the orientations picked randomly from a list of  $N$  choices. To ensure a particular area fraction of textured grains, the orientation list is composed so that  $N = N_r + N_t$ , where  $N_r$  is the number of orientations picked randomly from all of Euler space, and  $N_t$  is the number orientations picked randomly within  $5^\circ$  from the origin of the Euler space. Thus, fixing  $N_r = 36$ , we obtained an initial microstructure with cube texture fraction of 27% with  $N_t = 12$ , and another microstructure with a fraction of 12.5% by using  $N_t = 4$ . In the simulations, the area fractions of the cube grains are tracked and reported in the results.

For the purpose of studying the effect of dispersion of the textured grains on microstructural evolution, we have generated initial microstructures with three different dispersions of the textured grains: uniform, random and clustered. These microstructures and the corresponding MDFs are shown in Figs. 2(b)–(d) and 5(a), respectively. In the microstructures, randomly oriented grains (R-grains) are darkly shaded while textured grains (T-grains) are lightly shaded. The algorithm that we used to produce the initial dispersion is similar to the one employed by Miodownik et al. [17], which chooses two grains randomly and switches their orientations if the exchange reduces the difference between the resulting dispersion and the desired one. The MDF is measured in

terms of number fraction of grain boundaries of a specific range of misorientation. Using fraction of grain boundary arc length gives similar results. And in all the cases considered, both T-grains and R-grains have similar initial average grain size and lognormal size distributions.

The various dispersions of the T-grains shown in Fig. 2(b)–(d) can be represented qualitatively by different fractions of low-angle grain boundaries in the MDF curves. A higher fraction of low-angle boundaries represents a higher degree of clustering of the T-grains. Therefore, in addition to monitoring microstructural evolution and grain growth kinetics, both the dispersion of T-grains and the MDF are examined qualitatively through the fraction of low-angle grain boundaries. According to the spread of the orientations among the T-grains assumed in this study, the T–T boundaries are low-angle grain boundaries ( $<5^\circ$ ). Following the Mackenzie distribution, most boundaries between T- and R-grains (T–R boundaries) and between R-grains (R–R boundaries) are high-angle grain boundaries and essentially have similar properties. Therefore, the fraction of the T–T boundaries,  $f_{T-T}$ , is related directly to the fraction of low-angle grain boundaries in the MDF curves and hence represents the degree of clustering of the T-grains.

### 3. Results

The evolution of a random dispersion of textured grains (Fig. 2(c)), under anisotropy of boundary energy and mobility, is shown in Figs. 3 and 4, respectively. Comparing these results, one can readily see the difference in the fractions of the textured grains in the two cases. Fig. 5(b) shows quantitatively the evolution of area fraction of texture for all the cases considered. Clearly, the fraction of the texture component increases when energy is anisotropic, but texture decreases when mobility is anisotropic while energy is isotropic. Also, the growth of texture is a decelerating process, whereas texture reduction accelerates with time.

The initial dispersion of the T-grains plays an important role in determining the kinetics of texture development. The initial slopes of the texture evolution curves in Fig. 5(b) are listed in Table 1, and they vary significantly, depending on initial texture dispersion. Since the initial slopes for the cases with mobility anisotropy are very small, and therefore subject to greater error, the comparison is made primarily among systems with energy anisotropy. For a uniform initial dispersion, the texture fraction remains almost constant at early stages of annealing. Also, the random initial dispersion produces a higher initial growth rate of texture as compared to the clustered one.

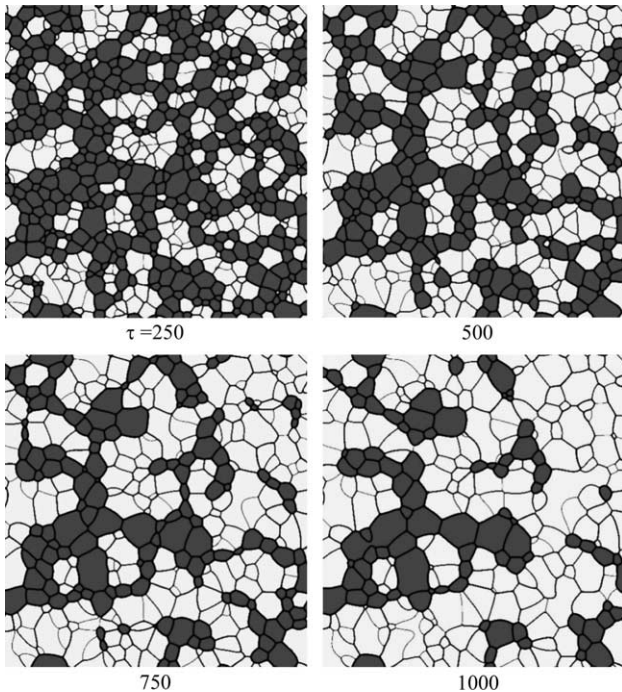


Fig. 3. Texture evolution during grain growth in a system consisting of 27% initially randomly distributed textured grains under the condition of anisotropic boundary energy and isotropic boundary mobility.  $\tau$  is reduced time.

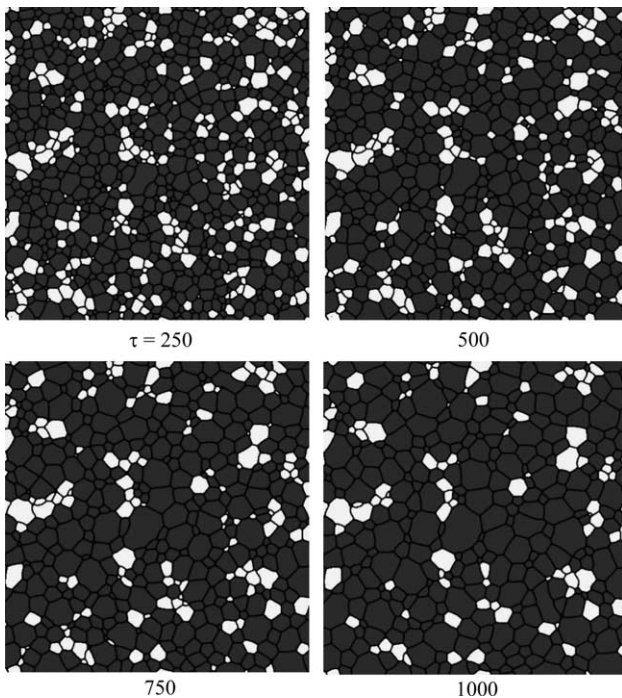


Fig. 4. Texture evolution during grain growth in a system consisting of 27% initially randomly distributed textured grains under the condition of anisotropic boundary mobility and isotropic boundary energy.  $\tau$  is reduced time.

The topological features of the polycrystalline microstructures obtained for energy anisotropy are also different from those obtained for mobility anisotropy. The dihedral angles at triple junctions maintain a value of  $2\pi/3$  when boundary energy is isotropic, but they may deviate significantly from  $2\pi/3$  when boundary energy is anisotropic. Low energy boundaries appear as lighter shades of gray in Fig. 3.

Fig. 5(c) shows the time-dependence of the number fraction of the T–T boundaries (low-angle boundaries),  $f_{T-T}$ , in various cases considered. The initial slopes of all the curves are positive, which means that the formation of T-grain clusters is inevitable for the assumed initial fraction of the texture component. Even when the starting microstructure contains only isolated T-grains, coarsening of the microstructure soon produces T-grain clusters. When boundary energy is anisotropic, the fraction of low-angle boundaries increases during grain growth. When boundary mobility is anisotropic but energy is isotropic, the fraction  $f_{T-T}$  increases initially and reaches a plateau before it starts to decrease slightly towards the end of the simulation, when the overall texture fraction decreases. Even when the boundary energy is isotropic, anisotropy in boundary mobility alone causes a variation of  $f_{T-T}$  with time, and hence a variation of MDF with time is expected. This result is different from previous observations [20,21] on systems with anisotropic mobility and isotropic energy, where the MDFs are time invariant. However, the time invariance of MDF was observed in microstructures that were either fully random or else fully textured, whereas the present microstructures contain textured grains in a matrix of randomly oriented grains.

Fig. 5(d) shows the average grain area as a function of time for all the cases studied. The curves are normalized by their initial slope for comparison. It is apparent that in all cases the grain growth kinetics deviates from that for isotropic grain growth where the average grain area grows linearly with time. These findings are also different from the results obtained in previous studies [20,21] for systems of either single-component texture or random texture but no mixture of the two, where it was shown that the mobility anisotropy alone does not alter grain growth kinetics. The non-linear growth of average grain area seems to be related to the fact that the MDF is no longer time-invariant in the current case. Quantitatively, the deviation from linear growth kinetics is more pronounced when boundary energy is anisotropic and becomes maximum when both energy and mobility are anisotropic because low energy boundaries have also low mobility according to the functions employed (Fig. 1). The degree of deviation from the linear area-time relation depends also on the initial dispersion of the T-grains.

To examine the possible effect of the initial fraction of the T-grains, another set of parallel simulations were

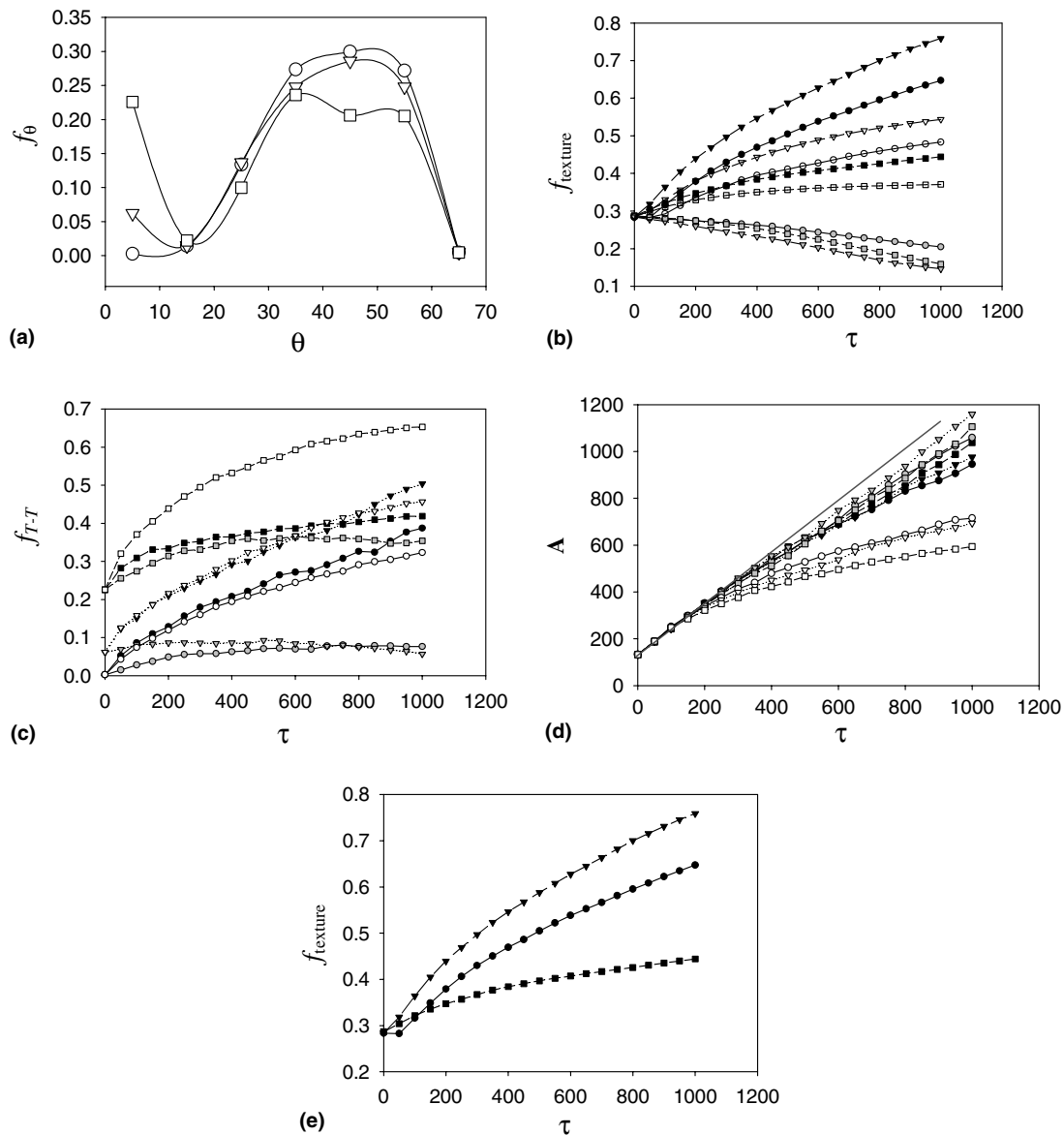


Fig. 5. (a) Initial MDFs, (b) temporal evolutions of area fractions of the texture component, (c) temporal evolution of number fraction of grain boundaries between textured grains and (d) temporal evolution of average grain area under various conditions with 27% initial texture component.  $\tau$  is reduced time. Circles, triangles and squares stand for uniform, random and clustered initial dispersion of texture component, respectively. Different shades of gray of the symbols represent various combinations of boundary properties, with solid, open and gray standing for energy anisotropy only, mobility anisotropy only and both energy and mobility anisotropy, respectively. The solid line in (d) is a straight line representing schematically parabolic grain growth kinetics. The three curves corresponding to energy anisotropy only in (b) are re-plotted in (e) to show clearly their initial slopes.

performed with 12.5% initial cubic texture. The results are presented in Fig. 6. The two initial fractions evolve similarly, which suggests that the results of the simula-

tions are qualitatively insensitive to the initial texture fraction in the range examined.

Table 1  
Initial slopes ( $\times 10^{-4}$ ) of curves shown in Fig. 5(b) for various combinations of anisotropy in boundary energy and mobility and spatial dispersions of the texture component

	Uniform	Random	Clustered
Energy anisotropy	0.6	8	4
Mobility anisotropy	-0.6	-0.8	-0.4
Energy + mobility anisotropy	0.2	4	3

#### 4. Discussion

The simulation results show that boundary energy anisotropy increases texture, whereas mobility anisotropy reduces it during grain growth, in a system comprising one texture component in a random matrix. When both energy and mobility are anisotropic, the fraction of the texture component increases but at

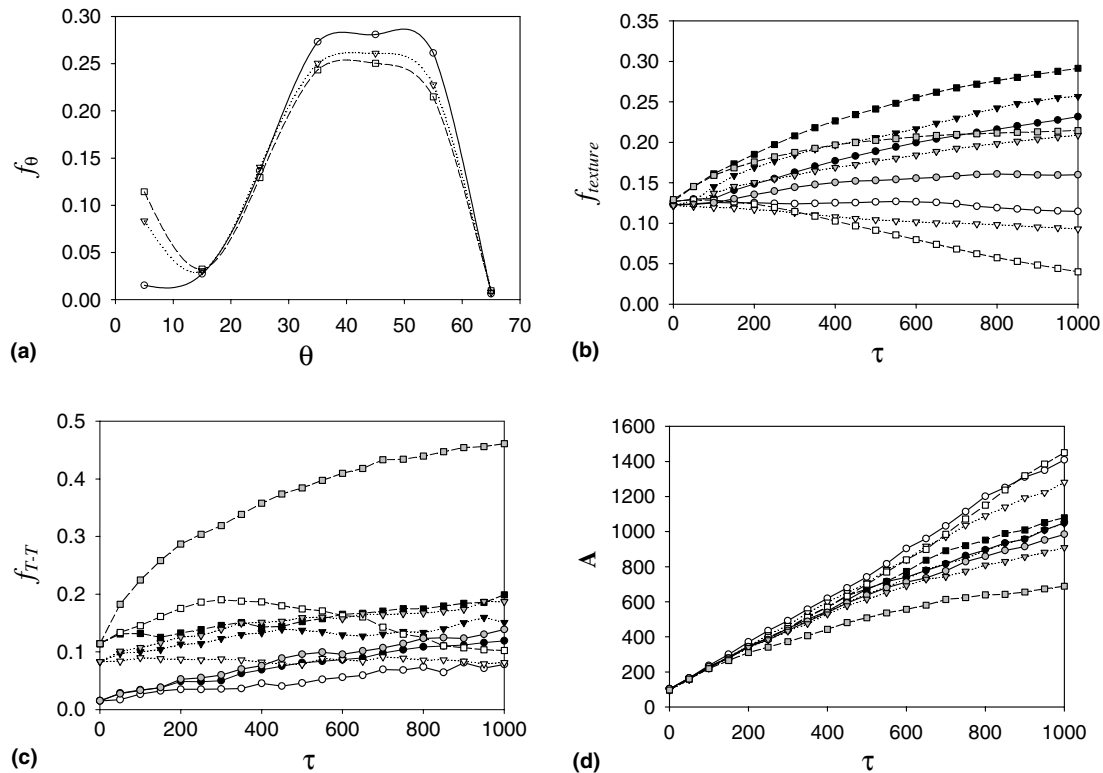


Fig. 6. (a) Initial MDFs, (b) temporal evolutions of area fractions of the texture component, (c) temporal evolution of number fraction of grain boundaries between textured grains and (d) temporal evolution of average grain area under various conditions with 12.5% initial texture component.  $\tau$  is reduced time. Circles, triangles and squares stand for uniform, random and clustered initial dispersion of texture component, respectively. Different shades of gray of the symbols represent various combinations of boundary properties, with solid, open and gray standing for energy anisotropy only, mobility anisotropy only and both energy and mobility anisotropy, respectively.

reduced rates. Qualitatively, these results are independent of the initial fraction and dispersion of the textured grains (T-grains). Quantitatively, however, the initial dispersion of the texture component plays an important role in determining the time-evolution of the misorientation distribution and hence affects the overall kinetics of texture evolution and grain growth.

It is apparent that all the factors considered in this study, and many others documented in the literature, play a role in texture evolution during grain growth. However, there are a large number of relevant factors and an even larger number of possible combinations, including boundary property anisotropy, initial dispersion and fraction of the texture component, the number of texture components present, and their average grain sizes and size distributions. Therefore, analysis of the results of a given study can be quite complicated, and disagreements of different studies can be difficult to resolve. However, as will be shown below, a key parameter that can be used as a general basis for analysis is the content of boundary energy density in a cluster of grains,  $\gamma/d$ , where  $\gamma$  is boundary energy and  $d$  is average grain size in the cluster. The same parameter was introduced by Turnbull [36] over half a century ago, to estimate the macroscopic driving force for grain growth.

Here, we use the relative magnitude of the  $\gamma/d$  potential in continuous clusters as a predictor of which cluster tends to grow and which tends to shrink.

#### 4.1. Effect of boundary mobility anisotropy

When a texture component exists in the initial microstructure, T–T boundaries will have, on average, much lower mobilities as compared to T–R or R–R boundaries. Thus, if the T-grains form clusters, which is inevitable during grain coarsening with the initial texture fractions considered, the grain size within a T-cluster will coarsen less rapidly than the surrounding matrix of R-grains. Therefore, as the microstructure evolves, the average grain size in a T-cluster will be smaller than that in an R-cluster. To illustrate this behavior, we plot the temporal evolutions of the microstructure and the grain size distributions of the T- and R-grains in Figs. 7 and 8, for the case of initially clustered dispersion. From Fig. 8, one can see that the initial size distributions of the T- and R-grains almost coincide with each other. As the microstructure evolves, however, the grain size distribution of the R-grains is shifted significantly towards larger grain sizes, resulting in the splitting of a single peak at  $\tau = 0$  into two peaks at a



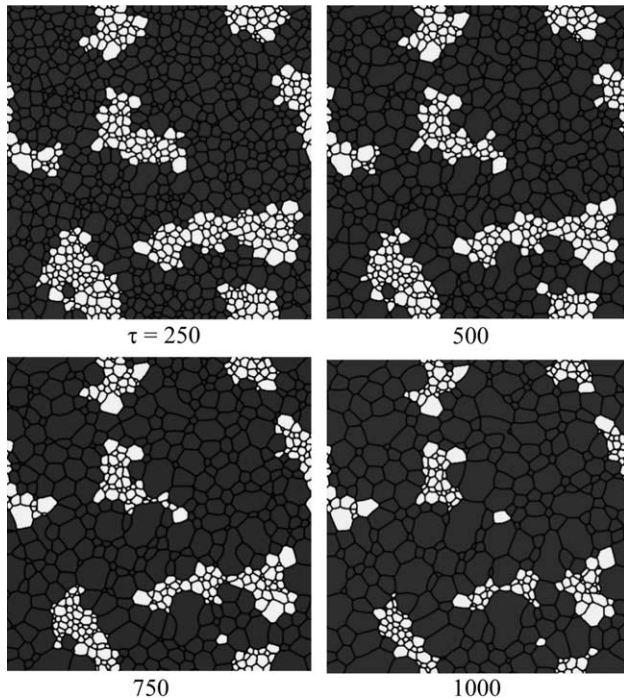


Fig. 7. Texture evolution during grain growth in a system consisting of 27% initially clustered texture component under the condition of anisotropic boundary mobility and isotropic boundary energy.  $\tau$  is reduced time.

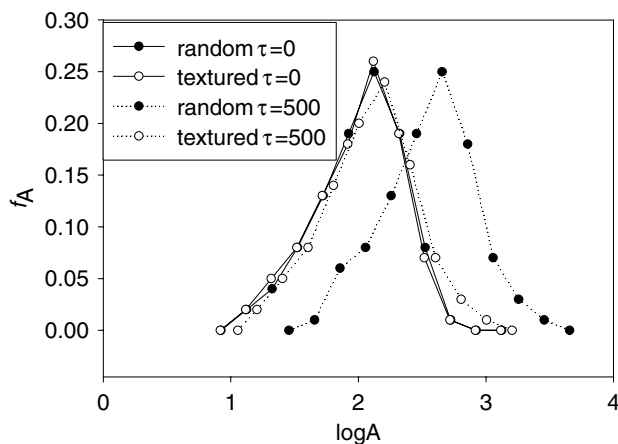


Fig. 8. Temporal evolution of grain size distributions of textured (open circles) and randomly oriented (solid circles) grains shown in Fig. 7.  $\tau$  is reduced time.

later time. The development of grain size disparity is also seen clearly in the microstructural evolution shown in Fig. 7. Since the grain boundary energy is isotropic, a T-grain cluster has a higher boundary energy density,  $\gamma/d$ , than the R-grain clusters. Therefore, the R-grains should grow at the expense of the T-grains, and hence, the fraction of the texture will decrease with time. Since the size difference between the T- and R-grains keeps increasing, the difference in the  $\gamma/d$  potential increases as

well, which accelerates the shrinkage of the T-grain clusters as shown in Figs. 5(b) and 6(b).

#### 4.2. Effect of boundary energy anisotropy

For the case of boundary energy anisotropy, the T–T boundaries have lower energies than the other higher misorientation boundaries in the system. Since the average grain size of the T- and R-grains are similar in the initial microstructure, a T-grain cluster will have lower  $\gamma/d$  potential than an R-grain cluster. Therefore, the T-grain clusters should grow at the expense of the R-grains. The preferential growth of texture clusters is quite evident from the concave T–R grain boundaries along the T-grain cluster perimeter (Fig. 9). This result agrees with the MC simulations by Hwang et. al. [13]. Note also that the dihedral angles at most of the T–T–R triple junctions deviate significantly from  $2\pi/3$ , with the dihedral angles on the R-grain sides close to  $\pi$ . As grains coarsen, the average grain size of the R-grains increases faster than that of the T-grains and the difference in the  $\gamma/d$  potentials between the T- and R-grain clusters will decrease. As a consequence, the growth of the T-grain clusters and hence the increase of the texture component should decelerate with time as shown in Fig. 5. If there are few T-grain clusters in the system such as in the case of uniform dispersion of the texture component, the

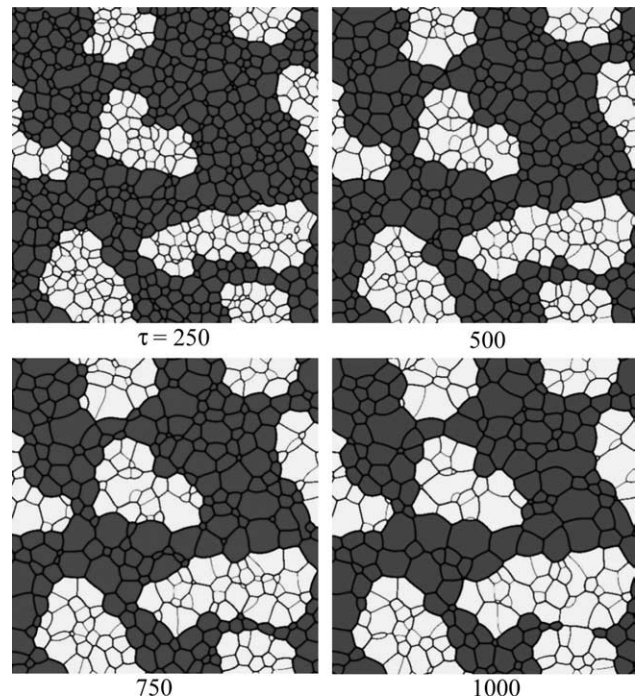


Fig. 9. Texture evolution during grain growth in a system consisting of 27% initially clustered texture component under the condition of anisotropic boundary energy and isotropic boundary mobility.  $\tau$  is reduced time.



initial growth rate of texture will be very small as shown in Table 1.

#### 4.3. Interplay between energy and mobility anisotropy

When both boundary energy and mobility are anisotropic, with low energy corresponding to low mobility, the effect of mobility anisotropy is to slow down grain growth within the T-grain clusters and hence lead to a higher  $\gamma/d$  potential than would be expected from energy anisotropy alone. This effect will reduce the difference in  $\gamma/d$  potentials of the two types of clusters during the evolution process, and it slows down the preferential growth rate of the texture component, as shown in Fig. 5(b). In the extreme case, e.g., when the mobility of the T–T grain boundaries vanishes, the  $\gamma/d$  potential of the R-grain clusters will eventually be lower than that of the T-grain clusters and the texture component will decrease thereafter. Thus, under the simultaneous and opposing influences of energy and mobility anisotropy, the fraction of texture could increase or decrease, depending on the functional forms of boundary energy and mobility and the spread of misorientation angles in the T-grains.

#### 4.4. Effect of dispersion of texture component

Clustering of T-grains increases the fraction of small-angle grain boundaries and enhances the effect of boundary energy or mobility anisotropy on texture development. The initial fraction and dispersion of the T-grains control the initial and subsequent clustering of the T-grains during grain growth. With similar dispersions, decreasing the fraction of the texture component reduces the possibility of clustering. This becomes evident by comparing the texture development in the systems of 12.5% and 27% texture component. A smaller fraction of texture leads to fewer T-grain clusters and slower kinetics of texture evolution.

In addition to single-boundary properties, the rate of texture development and the overall grain growth kinetics depend quantitatively on the number of T-grain clusters, as well as their sizes, shapes and interconnectivity. For example, with the same initial area fraction and average grain size of the texture component, the random dispersion of the texture grains yields the maximum growth rate of the texture fraction,  $f_{\text{texture}}$ , and the clustered dispersion yields the minimum growth rate, when boundary energy is anisotropic, as shown in Table 1. Preferential growth of the T-grain clusters takes place at the cluster perimeter, where the disparity in  $\gamma/d$  represents an imbalance in the local forces acting at triple junctions. The total perimeter length of the T-grain clusters is greatest in the case of random dispersion, where the clusters percolate quickly through the microstructure. For uniform dispersion the total length

of the T-grain cluster perimeter is minimum at the beginning, but it gradually outgrows the case of clustered dispersion. Therefore, the growth rate of  $f_{\text{texture}}$  for the case of uniform dispersion is minimum at the beginning and gradually increases and eventually exceeds the case of clustered dispersion. However, the relatively slow growth of texture in the case of initially clustered grains is due in part to the compactness (convexity) of the clusters and their being well separated from one another. Therefore, the quantitative differences shown by the simulations of different initial dispersions may not be universally applicable, but the results show nonetheless that the details of initial dispersion have an important influence on the kinetics of texture development.

#### 4.5. Effect of grain size

It should be emphasized that the main conclusion on the effect of boundary energy anisotropy in increasing texture is valid only for the specific initial microstructures considered. If the T- and R-grains had different average grain sizes to start with, the grain boundary energy density ( $\gamma/d$ ) in the T-grain clusters could be higher than that in the R-grain clusters and hence the texture component could decrease rather than increase even if the boundary energy is anisotropic. This has been confirmed by the simulation results shown in Fig. 10, where two regular honeycomb microstructures of different grain sizes to start with, the grain boundary energy density ( $\gamma/d$ ) in the T-grain clusters could be higher than that in the R-grain clusters and hence the texture component could decrease rather than increase even if the boundary energy is anisotropic. This has been confirmed by the simulation results shown in Fig. 10, where two regular honeycomb microstructures of different grain sizes are considered. In the two parallel simulations, Fig. 10(a)–(d), the ratio of grain boundary energy of the two honeycomb microstructures has been fixed to 2, while the ratio of the grain sizes of the two

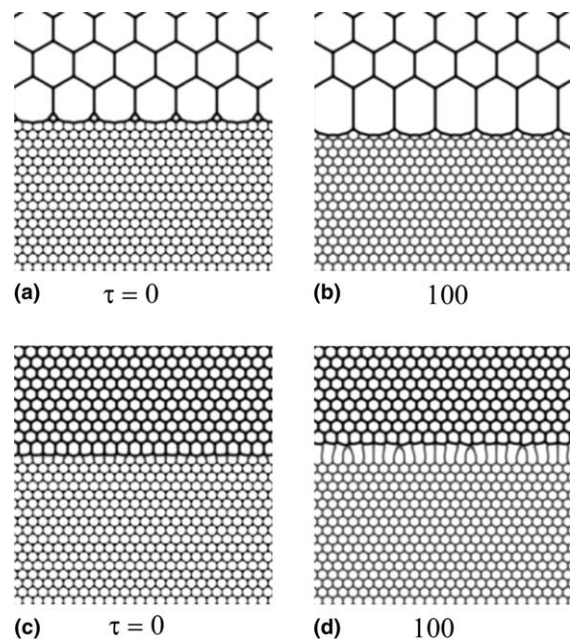


Fig. 10. Effect of initial grain size on microstructure evolution in a system consisting of two honeycomb structures.  $\tau$  is reduced time.

honeycomb microstructures have been chosen as 4 and 1.2, respectively. Therefore, in the former the “texture component” (the smaller grains that have lower boundary energy) has a higher  $\gamma/d$  potential, while in the latter the texture component has a lower  $\gamma/d$  potential. As a consequence, the texture component decreases in the former and increases in the latter. Such a situation could also be reached from coarsening of T- and R-grains of similar initial size distribution if the mobility of the T–T boundaries is much lower than that of the T–R and R–R boundaries, as has been discussed earlier in Section 4.3.

The main conclusion drawn on the effect of boundary mobility anisotropy on texture evolution, i.e., boundary mobility anisotropy reduces texture component during grain growth, however, holds irrespective of grain sizes. Suppose that the average grain size of the T-grains is larger than that of the R-grains in the initial microstructure. The T-grain clusters will grow at the expense of the surrounding R-grains at the beginning. However, since grains in the T-grain clusters will coarsen much slower than those in the R-grain clusters, eventually the average grain size of the R-grain clusters will exceed that of the T-grain clusters, leading to a lower  $\gamma/d$  potential for the R-grain clusters. Therefore, the texture component will eventually shrink under mobility anisotropy.

#### 4.6. Effect of number of texture component

In the current study, a single texture component embedded in a matrix of randomly oriented grains is considered. The simulation results show monotonic increase or decrease of the texture component, which is different from previous work on a mixture of two texture components [14–16,22] where an oscillation in the fractions of the two texture components has been predicted. However, this oscillation in texture can also be explained by applying the same argument of the  $\gamma/d$  potential. For example, in an initial microstructure consisting of two texture components of similar average grain sizes and size distributions but different volume fractions, the texture component of smaller volume fraction will be embedded in a matrix of the major component and hence has more A–B (high mobility) boundaries per unit volume. As the microstructure evolves, the average grain size of the minor component will exceed that of the major component and hence yield a lower value of  $\gamma/d$ . Then the minor component will grow at the expense of the major component at an accelerating rate till a moment when all the original matrix grains of greater values of  $\gamma/d$  are consumed and only locally small pockets of lower values of  $\gamma/d$  left (because grains do not have the same size). Then these small pockets will become the new minor component of lower  $\gamma/d$  and the process will be reversed.

#### 4.7. Texture effect on grain growth kinetics

If the entire microstructure has either random or single-component texture, the  $\gamma/d$  potential becomes uniform. In this case it has been shown previously [20,21] that grain growth in systems of isotropic boundary energy but anisotropic mobility behaves exactly the same as in an isotropic system: the MDF is time-invariant and the average grain area increases linearly with time. This is not true anymore for systems consisting of mixtures of R- and T-grains where  $\gamma/d$  potential is non-uniform. As analyzed earlier, the fraction of the texture component will either increase or decrease in this case, leading to a time-dependent MDF. According to [37], the grain growth kinetics will deviate from the parabolic law derived for isotropic systems. For systems of both boundary energy and mobility anisotropy, high-energy boundaries will be eliminated first during grain coarsening. Because the low energy boundaries have low mobility as well, which accelerates the selective elimination process of the high-energy boundaries, the negative deviation from linear growth kinetics become more severe (Fig. 5(d)).

For systems with mobility anisotropy only, the fraction of low mobility T–T boundaries decreases as T-grain clusters shrink, as shown in Fig. 7. In this case, an acceleration of the overall grain growth is expected. This behavior can also be found in Fig. 6(d).

### 5. Summary

The individual and combined effects of anisotropy in grain boundary energy and mobility, and dispersion and fraction of texture component on texture evolution during grain growth are investigated by computer simulations using the phase-field method. The systems considered consist of a single cube component embedded in a matrix of randomly oriented grains in the initial microstructure. Even though all the factors considered affect texture evolution, it is found that the key parameter that controls texture evolution is the grain boundary energy density characterized by  $\gamma/d$ . The fraction of the texture component increases when  $\gamma/d$  of the texture clusters is smaller than that of the randomly oriented grains, and decreases when  $\gamma/d$  of the textured grains is greater than that of the randomly oriented grains. The individual factors considered affect texture development through their influences on the  $\gamma/d$  potentials of the textured and randomly oriented grains. Their individual and combined effects on the  $\gamma/d$  potentials and hence on texture evolution and grain growth kinetics are analyzed and are found agree well with the simulation results.

Clustering of textured grains is inevitable during grain coarsening. The degree of clustering depends on the initial dispersion of the textured grains. Clustering causes

an increase in the fraction of low-angle boundaries in a system and, hence, alters the misorientation distribution function (MDF). As a consequence, initial microstructures of different degrees of clustering of textured grains are associated with different time-evolutions of the MDF and hence different grain growth kinetics.

### Acknowledgements

This work is supported by the US Air Force through the Metals Affordability Initiative under contract F33615-99-2-5215 and by the US AFOSR through the MEANS program under contract F49620-02-1-0056 with Dr. Craig Hartley as Program Manager. The authors thank for helpful discussion with Dr. A.D. Rollett in CMSN workshop.

### References

- [1] Sutton AP, Balluffi RW. *Interfaces in crystalline material*. New York: Oxford University Press; 1995.
- [2] Gottstein G, Shvindlerman LS. *Grain boundary migration in metal*. New York: CRC Press LLC; 1999.
- [3] Hu H, Cline RS, Goodman SR. Recrystallization, deformation textures of metals. In: *grain growth and texture*. Metal Park, OH: ASM; 1965. p. 295.
- [4] Humphreys FJ, Hatherly M. *Recrystallization and Related Annealing Phenomena*. New York: Elsevier Science; 1995.
- [5] Palumbo G, Lehooky EM, Lin P, Erb U, Avst KT. *Mater Res Soc Symp Proc* 1997;458:273.
- [6] Palumbo G, Lehooky EM, Lin P. *JOM* 1998;50(2):40.
- [7] Watanabe T, Tsurekawa S. *Acta Mater* 1999;47:4171.
- [8] Watanabe T. *Mater Sci Forum* 2002;408–412:39.
- [9] Adams BL, Wright SI, Kunze K. *Metall Trans A* 1993;24:819.
- [10] Ono N, Kimura K, Watanabe T. *Acta Metall* 1999;47:1007.
- [11] Grest GS, Srolovitz DJ, Anderson MP. *Acta Metall* 1985;33:509.
- [12] Rollett AD, Srolovitz DJ, Anderson MP. *Acta Metall* 1989;37:1227.
- [13] Hwang NM, Lee BJ, Han CH. *Scripta Mater* 1997;37:1761.
- [14] Mehnert K, Klimanek P. *Comput Mater Sci* 1996;7:103.
- [15] Mehnert K, Klimanek P. *Comput Mater Sci* 1997;9:261.
- [16] Ivasishin OM, Shevchenko SV, Vasiliev NL, Semiatin SL. *Acta Mater* 2003;51:1019.
- [17] Miodownik M, Godfrey AW, Holm EA, Hughes DA. *Acta Mater* 1999;47:2661.
- [18] Holm EA, Hassold GN, Miodownik MA. *Acta Mater* 2001;49:2981.
- [19] Rollett AD. *Mater Sci Forum* 2002;408–4:251.
- [20] Kazaryan A, Wang Y, Dregia SA, Patton BR. *Acta Mater* 2002;50:2491.
- [21] Upmanyu M, Hassold GN, Kazaryan A, Holm EA, Wang Y, Patton BR, et al. *Interface Sci* 2002;10:201.
- [22] Abbruzzess G, Lücke K. *Acta Metall* 1986;34:905.
- [23] Novikov VY. *Acta Mater* 1999;47:1935.
- [24] Humphreys FJ. *Acta Mater* 1997;45:4231.
- [25] Hillert M. *Acta Metall* 1965;13:227.
- [26] Chen LQ. *Scripta Met* 1995;32(1):115.
- [27] Kazaryan A, Wang Y, Dregia SA, Patton BR. *Phys Rev B* 2000;61:14275.
- [28] Kabayashi R, Warren JA, Carter WC. *Physica D* 2000;140:141.
- [29] Warren JA, Kobayashi R, Lobkovsky AE, Carter WC. *Acta Mater* 2003;51:6035.
- [30] Bunge HJ. *Texture analysis in materials science*. London Press; 1982.
- [31] Mackenzie JK, Thomson M. *Biometrika* 1957;44:205.
- [32] Mackenzie JK. *Biometrika* 1958;45:229.
- [33] Cahn JW, Hillard JE. *J Chem Phys* 1958;28:258.
- [34] Read WT, Shockley W. *Phy Rev* 1950;78:275.
- [35] Huang Y, Humphreys HJ. *Acta Metall* 2000;48:2017.
- [36] Turnbull D. *Trans Metall Soc AIME* 1951;191:661.
- [37] Kazaryan A, Patton BR, Dregia SA, Wang Y. *Acta Mater* 2002;50:499.